Received: 18 December 2024 | Revised: 25 April 2025 | Accepted: 15 May 2025

DOI: 10.1002/alz.70367

Alzheimer's & Dementia®
THE JOURNAL OF THE ALZHEIMER'S ASSOCIATION

RESEARCH ARTICLE

Structural and functional connectivity in tau mutation carriers: from presymptomatic to symptomatic frontotemporal dementia

Arabella Bouzigues[1,2] | Vincent Le Du[1] | Matthieu Joulot[1] | Ninon Peysson[1] | Marion Houot[1,3] | Benoît Béranger[1] | Lucy L. Russell[2] | Phoebe H. Foster[2] | Eve Ferry-Bolder[2] | John C. van Swieten[4] | Lize Jiskoot[4] | Harro Seelaar[4] | Raquel Sanchez-Valle[5] | Robert Laforce[6] | Caroline Graff[7,8] | Daniela Galimberti[9,10] | Rik Vandenberghe[11,12,13] | Alexandre de Mendonça[14] | Pietro Tiraboschi[15] | Isabel Santana[16,17] | Alexander Gerhard[18,19,20] | Johannes Levin[21,22,23] | Sandro Sorbi[24,25] | Markus Otto[26] | Maxime Bertoux[27] | Thibaud Lebouvier[27] | Simon Ducharme[28,29] | Chris R. Butler[30,31] | Isabelle Le Ber[1,3] | Elizabeth Finger[32] | Maria Carmela Tartaglia[33] | Mario Masellis[34] | James B. Rowe[35] | Matthis Synofzik[36] | Fermin Moreno[37,38,39] | Barbara Borroni[40,41] | Jonathan D. Rohrer[2] | Raffaella Migliaccio[1,3] | the GENetic Frontotemporal dementia Initiative (GENFI)

Correspondence
Arabella Bouzigues, Paris Brain Institute, Sorbonne Université, INSERM U1127, Hôpital Pitié-Salpêtrière, Paris, France.
Email: arabella.bouzigues.18@ucl.ac.uk

Raffaella Migliaccio, Paris Brain Institute & IM2A, Hôpital Pitié-Salpêtrière, Paris.
Email: lara.migliaccio@gmail.com

Abstract

INTRODUCTION: Microtubule-associated protein tau (*MAPT*) mutations cause frontotemporal dementia (FTD), characterised by behavioural, language, and motor impairments due to brain connectivity disruptions. We investigated structural and functional connectivity in 86 mutation carriers and 272 controls to map connectivity changes at different disease stages.

METHODS: The CDR Dementia Staging Instrument plus National Alzheimer's Coordinating Center (NACC) Behaviour and Language domains (CDR plus NACC FTLD)

Funding information: Fondation Recherche Alzheimer; Dioraphte Foundation, Grant/Award Number: 09-02-03-00; Association for Frontotemporal Dementias Research, Grant/Award Number: 2009; Netherlands Organization for Scientific Research, Grant/Award Number: HCMI 056-13-018; Deltaplan Dementie, Grant/Award Number: 733 051 042; ZonMw Onderzoeksprogramma Dementie, Grant/Award Number: 10510032120002; Alzheimer Nederland; Alzheimer's Research UK Clinical Research, Grant/Award Number: ARUK-CRF2017B-2; Fundació Marató de TV3, Grant/Award Number: 20143810; Neurodegenerative Disease Research-Prefrontals Vetenskapsrådet Dnr, Grant/Award Number: 529-2014-7504; Neurodegenerative Disease Research-GENFI-PROX; Vetenskapsrådet, Grant/Award Number: 2018-02754; FTD Inititative-Schörling Foundation; Alzheimer Foundation; Brain Foundation; Dementia Foundation; Neurodegenerative Disease Research and the Italian Ministry of Health (PreFrontALS), Grant/Award Number: 733051042; Mady Browaeys; Research into Frontotemporal Dementia; Deutsche Forschungsgemeinschaft German Research Foundation; Germany's Excellence Strategy within the framework of the Munich Cluster for Systems Neurology, Grant/Award Number: EXC 2145 SyNergy—ID 390857198; Germany's Federal Ministry of Education and Research (BMBF); Canadian Institute of Health Research, Grant/Award Number: 327387; Canadian Institute of Health Research operating; Weston Brain Institute and Ontario Brain Institute; Wellcome Trust, Grant/Award Numbers: 103838, 220258; Bluefield Project; Cambridge University Centre for Frontotemporal Dementia; Medical Research Council, Grant/Award Numbers: MC_UU_00030/14, MR/T033371/1; National Institute for Health Research Cambridge Biomedical Research Centre, Grant/Award Number: NIHR203312; Tau Consortium; Carlos III Health Institute, Grant/Award Number: PI19/01637; University College London Hospitals Biomedical Research Centre; MRC Clinician Scientist Fellowship, Grant/Award Number: MR/M008525/1; Miriam Marks Brain Research UK; France Alzheimer; Fondation Recherche Alzheimer; Fondation Philippe Chatrier; European Reference Network for Rare Neurological Diseases (ERN-RND), Grant/Award Number: No. 739510; Neurodegenerative Disease Research GENFI-PROX, Grant/Award Number: 2019-02248; Association pour la Recherche sur la Sclérose Latérale Amyotrophique et autres Maladies du Motoneurone; Fondation Vaincre Alzheimer; National Institute for Health and Care Research; Rosita Gomez association; Region Stockholm ALF-project

stratified carriers into three groups: asymptomatic, prodromal, and symptomatic. We extracted measures of cortical thickness, white matter integrity, and functional connectivity, which were compared between each carrier group and controls using linear mixed models.

RESULTS: Early isolated functional disruptions in salience/visual networks were present in asymptomatic carriers, along with anterior cingulate gray matter reductions. In prodromal carriers, functional changes extended to other networks, with additional structural damage in temporal poles/cingulate.

DISCUSSION: This study shows that functional networks likely drive lifelong compensation for a genetically determined disease, manifesting clinically when structural damage reaches a critical threshold. This supports connectivity measures as potential biomarkers for *MAPT*-related neurodegeneration.

KEYWORDS
functional connectivity, genetic frontotemporal dementia, graph analysis, gray matter, macroscale organization, MAPT, mutation, neurodegeneration, tau, tau pathology, white matter

Highlights

- Our findings reveal the progressive and staged nature of structural and functional connectivity alterations in *MAPT* mutation carriers, with distinct patterns at each disease stage.
- In asymptomatic carriers, we identified early functional connectivity alterations in salience and visual networks, despite preserved white matter and only subtle gray matter atrophy. These appear to represent both response to pathology and possible compensatory mechanisms.
- In prodromal carriers, functional connectivity alterations were accompanied by structural damage, including cortical atrophy and white matter tract disruptions, in regions directly connected to early-affected networks.
- The sequential progression, from functional connectivity changes to structural degeneration, aligns with the hypothesis that tau propagates along axonal connections, disrupting neural network integrity before measurable atrophy occurs.
- We propose a theoretical data-driven model of biomarker evolution in *MAPT* mutation carriers, highlighting functional disruptions as early indicators and structural damage as a later-stage hallmark.
- These connectivity biomarkers have the potential to inform therapeutic strategies and clinical trial design.

1 | BACKGROUND

Many mutations in the microtubule-associated protein tau (*MAPT*) gene are pathogenic and known to lead to frontotemporal dementia (FTD), neurodegenerative conditions primarily affecting behaviour, language, and/or motor function.[1,2] *MAPT* mutation carriers often develop the behavioural variant of FTD (bvFTD), characterised by behavioural and personality deterioration, but also other clinical manifestations such as corticobasal syndrome (CBS), progressive supranuclear palsy (PSP), or an Alzheimer's-like syndrome.[2] Subjects with *MAPT* mutations typically exhibit an earlier age of symptom onset compared to carriers of other gene mutations like expansions in C9 open reading-frame 72 (*C9orf72*) or progranulin (*GRN*), sometimes as early as in the second decade of life.[3–5]

Neurodegenerative syndromes like FTD are thought to reflect the disruption of large-scale neuronal networks, with both structural and functional connectivity changes reported in patients.[6–17] Research suggests that the progression of these diseases may arise from the

propagation of pathological processes along anatomical and functional brain connectivity pathways.[18–21] A key challenge in the field is understanding how tau pathology spreads from its initial site of aggregation. Some studies propose that tau aggregates propagate to neighbouring brain regions,[22] while others suggest that tau spreads along synaptically connected networks.[23]

Although several studies have explored connectivity changes in *MAPT* mutation carriers, research is often limited by small sample sizes, and few studies have examined both structural and functional connectivity simultaneously. This gap hinders a comprehensive understanding of these two types of connectivity and their changes at different disease stages. Some evidence suggests that in *MAPT* mutation carriers, functional connectivity changes in frontotemporal circuits may precede structural atrophy.[9,24] Metabolism studies also highlight altered connectivity before detectable structural neurodegeneration occurs.[25–27] These early functional changes have also been reported to show patterns of change opposite to those seen in patients, possibly reflecting synaptic dysfunction related to tau pathology or compensatory mechanisms, suggesting potential as biomarkers for disease progression.[26,28]

The primary aim of this study was to identify which connectivity pathways become altered and when during the disease course in *MAPT* mutation carriers, shedding light on the molecular processes underlying neurodegeneration. Structural connectivity was assessed via cortical thickness and white matter (WM) tract integrity, while functional connectivity was examined through graph theory measures (local and global) and macroscale gradients of functional networks. Furthermore, we stratified *MAPT* mutation carriers into three groups, accounting not only for asymptomatic versus symptomatic status but also for the "grey zone" representing the transitional phase between these stages, defined here as "prodromal." Consistent with the existing literature, we hypothesised that changes in functional networks would be detectable from the earliest presymptomatic stages, whereas structural alterations would be more closely linked to symptom onset. Understanding these changes may enhance our knowledge of FTD pathology progression and contribute to the identification of biomarkers for early diagnosis, accurate staging, and effective disease monitoring.

RESEARCH IN CONTEXT

1. **Systematic review**: This study builds on a growing body of literature investigating the neural correlates of tau-related neurodegeneration, specifically in the context of *MAPT* mutations associated with FTD. Neurodegeneration such as that involved in *MAPT*-related FTD involves the disruption of large-scale neuronal networks, with the propagation of pathological processes occurring along anatomical and functional brain connectivity pathways. A review of prior work informed the selection of advanced structural and functional imaging approaches and guided the definition of a well-characterised cohort of *MAPT* mutation carriers to better understand the mechanisms of pathology progression by identifying which connectivity pathways become altered and when during the disease course.
2. **Interpretation**: Our findings demonstrate that functional network alterations emerge early in the disease process, preceding or co-occurring with structural damage in *MAPT*-associated FTD. These results support a model in which tau pathology disrupts large-scale brain networks early on, with subsequent structural degeneration reflecting a progression of these functional abnormalities. Additionally, the data suggest a dynamic interplay between pathological changes and potential compensatory mechanisms. Together, these insights highlight the importance of both functional and structural connectivity biomarkers in improving early diagnosis, disease staging, and therapeutic monitoring in tauopathies.
3. **Future directions**: While clinical trials are under way for several forms of genetic FTD, *MAPT* mutation carriers remain underrepresented in therapeutic development efforts. Future research must prioritise the validation of robust and reliable biomarkers specifically tailored to this population. Longitudinal studies with larger cohorts are needed to confirm the temporal sequence of network changes and to assess their predictive value for clinical progression. Additionally, future trials will benefit from identifying biomarkers that are not only sensitive to disease onset and progression but also responsive to therapeutic intervention, thereby accelerating the path toward targeted treatment strategies for tauopathies.

2 | METHODS

2.1 | Participants

We included controls ($n = 272$) and *MAPT* mutation carriers ($n = 86$) from the sixth data freeze in the GENFI study. These participants completed a baseline visit between January 2012 and January 2021 across 24 centers in the United Kingdom, Canada, Italy, the Netherlands, Sweden, Portugal, Germany, France, Spain, and Belgium. The study was approved by each local ethics committees, written informed consent was obtained from all participants, and the study was conducted in accordance with the ethical standards of the Declaration of Helsinki. Participants were screened and genotyped at their local sites. *MAPT* mutations included mutations in intron 10 (IVS10+14, IVS10+15A > C, IVS10+16, IVS10+16C > T, IVS10+3G > A, IVS10+16) as well as exonic missense mutations (G272V, L266V, L315R, P301L, P397S, Q351R, R406W, S320F, S356T). GENFI has strict eligibility criteria that includes only the inclusion of participants with confirmed pathogenic mutations. The distribution of mutations across our *MAPT* carrier groups is detailed in Table S1. All participants underwent a standard-

TABLE 1 Demographic and neuropsychological details of sample studied, with values presented as mean ± standard deviation, unless otherwise noted.

Demographic data	*MAPT* carriers						
FTLD-CDR global score	0 = asymptomatic		0.5 = prodromal		1 to 3 = symptomatic		Controls
N	47		16		23		272
Sex ratio F:M	28:19	*n.s.*	09:07	*n.s.*	08:15	*n.s.*	163:118
Age (years)	39.7 ± 11.0	*0.003*	42.2 ± 11.5	*n.s.*	56.4 ± 10.0	*0.0001*	45.8 ± 13.0
Education (years)	14.6 ± 3.3	*n.s.*	14.3 ± 2.4	*n.s.*	14.1 ± 3.4	*n.s.*	14.5 ± 3.4
MMSE	28.3 ± 6.1	*n.s.*	26.7 ± 7.4	*n.s.*	23.0 ± 7.1	*<0.0001*	28.9 ± 4.1
Neuropsychological data							
Benson figure recall	12.5 ± 3.9	*n.s.*	12.3 ± 5.0	*n.s.*	6.1 ± 4.8	*<0.0001*	12.9 ± 3.5
Camel and cactus	28.0 ± 8.2	*n.s.*	29.7 ± 2.6	*n.s.*	25.1 ± 3.9	*<0.0001*	29.3 ± 5.8
Trail Making Test A time	23.1 ± 10.3	*n.s.*	23.4 ± 5.4	*n.s.*	41.2 ± 17.1	*<0.0001*	26.6 ± 12.8
Trail Making Test B time	53.8 ± 23.4	*0.03*	59.1 ± 23.5	*n.s.*	133.1 ± 71.8	*<0.0001*	62.2 ± 33.6
Boston Naming Test	27.4 ± 4.5	*n.s.*	27.1 ± 3.2	*n.s.*	16.6 ± 6.9	*<0.0001*	27.4 ± 4.2
FCSRT immediate free	27.7 ± 12.1	*n.s.*	30.3 ± 10.6	*n.s.*	11.1 ± 8.2	*<0.0001*	30.3 ± 8.6
FCSRT immediate total	40.2 ± 15.7	*n.s.*	43.1 ± 8.3	*n.s.*	25.7 ± 10.8	*<0.0001*	43.8 ± 9.0
FCSRT delayed free	10.5 ± 4.9	*n.s.*	10.8 ± 4.8	*n.s.*	4.1 ± 3.9	*0.0001*	11.7 ± 3.4
FCSRT delayed total	13.4 ± 5.4	*n.s.*	14.5 ± 3.2	*n.s.*	9.3 ± 4.1	*<0.0001*	15.0 ± 3.1
Stroop ink time	47.0 ± 20.2	*n.s.*	46.0 ± 9.8	*n.s.*	85.0 ± 35.8	*0.001*	50.4 ± 15.8
Verbal fluency animals	23.3 ± 7.4	*n.s.*	23.4 ± 5.8	*n.s.*	13.4 ± 6.2	*<0.0001*	23.7 ± 6.7
Verbal fluency F	13.8 ± 5.7	*n.s.*	14.8 ± 4.7	*n.s.*	9.0 ± 5.3	*0.0002*	13.4 ± 5.2
Verbal fluency A	12.4 ± 5.3	*n.s.*	12.7 ± 4.8	*n.s.*	7.1 ± 4.6	*<0.0001*	12.3 ± 4.9
Verbal fluency S	13.7 ± 5.8	*n.s.*	16.6 ± 6.0	*0.04*	9.4 ± 4.0	*0.0002*	13.6 ± 5.6
miniSEA	23.1 ± 8.1	*n.s.*	24.5 ± 2.9	*n.s.*	19.1 ± 7.0	*0.01*	25.1 ± 4.7

The column to the right of the values is the result of statistical comparisons with control group; the *p* value is reported if there was no significant difference; *n.s.* is reported.

Abbreviations: FCSRT, Free and Cued Selective Reminding Test; FTLD-CDR, Clinical Dementia Rating scale plus National Alzheimer's Coordinating Center Behaviour and Language domains; *MAPT*, microtubule-associated protein tau; *n.s.*, non-significant.

ised clinical assessment as described previously,[29] including the CDR Dementia Staging Instrument plus National Alzheimer's Coordinating Center (NACC) Behaviour and Language domains (CDR plus NACC FTLD), hereafter referred to as FTLD-CDR,[30] a measure of disease severity from which a global score can be calculated. The global score was used in this work to stage mutation carriers, with those having a score of 0 being considered asymptomatic, 0.5 as prodromal, and 1, 2, or 3 as symptomatic. We compared demographic details and neuropsychological test scores across multiple cognitive domains between each carrier group and controls, using chi-squared tests for sex and Kruskal-Wallis followed by Mann–Whitney U tests for continuous variables. Our sample's characteristics are summarized in Table 1.

2.2 | Neuroimaging sequences

Analogous imaging sequences were acquired on 3T magnetic resonance imaging (MRI) scanners at each GENFI site accommodating different manufacturers. A summary of the different scanners used and the specific protocol parameters for each can be found in Table S2.

For anatomical images, T1-weighted scans were acquired using a magnetisation prepared rapid acquisition gradient echo pulse sequence (MPRAGE). T2*-weighted echo-planar imaging (EPI) pulse sequences for resting-state functional MRI (fMRI) were acquired for functional imaging. Participants were asked to lie with their eyes closed, without falling asleep, during the resting-state acquisition run. Finally, diffusion-weighted scans were acquired using single-shell diffusion encoding with a b-value of 1000 s/mm^2 and 64 diffusion directions. Data were collected using single-shot spin-echo echo-planar imaging (SE-EPI) with interleaved acquisitions of five non-diffusion-weighted (b = 0) images.

2.3 | Gray matter analysis

2.3.1 | Preprocessing

T1 scans that passed visual quality inspection were processed using FreeSurfer version 7.1.1. This pipeline performs cortical surface extraction, segmentation of subcortical structures, cortical thickness esti-

mation, spatial normalisation onto the FreeSurfer surface template (FsAverage), and parcellation of cortical regions based on different atlases.[31] We ran the recon-all cross-sectional analysis using Clinica's t1-freesurfer pipeline.[32] FreeSurfer segmentation outputs were each visually inspected for serious errors. When serious errors occurred, or when FreeSurfer crashed without providing outputs and this was not fixed by repeated attempts, FreeSurfer analyses of those scans were omitted. No manual correction of FreeSurfer segmentations was performed.

2.3.2 | Cortical thickness extraction

Gray matter (GM) thickness values were generated using the recon-all cross-sectional approach, which generated values across 327,684 vertices of the cortex, with a full width at half maximum of 20. FreeSurfer is a surface-based analysis (SBA), meaning that for each vertex, cortical thickness is calculated as the mean distance between vertices of a corrected, triangulated, estimated GM/WM surface and GM/cerebrospinal fluid (CSF) (pial) surface.[33]

2.4 | WM connectivity analysis

2.4.1 | Preprocessing

Diffusion-weighted images (DWI) were preprocessed using an in-house pipeline that combines state-of-the-art tools (DWEZ).[34] The overall steps involved, first, concatenation and denoising of the DWI volumes, followed by removing Gibbs ringing artifacts using MRtrix3 tools. Then we performed motion correction with FSL's mcflirt, extracted a mean b = 0 image, and stripped the skull from the T1 image using SynthStrip, a Python singularity wrapper. Next, using Synb0-DISCO, a deep-learning tool, we generated a synthetic undistorted b = 0 volume, which was input into FSL topup for DWI distortion correction. Finally, a new mean b = 0 was extracted from the undistorted DWI volumes from which SynthStrip created a new brain mask. Tissue response, fiber orientation distribution, and tissue segmentation on the aligned DWI to T1w scan, followed by anatomical constrained tractography (ACT), were performed using MRtrix3.

Further details regarding this pipeline can be found in the openly available repository: https://github.com/Vince-LD/DWEZ.

2.4.2 | Segmentation and data extraction

To extract WM bundles, we used TractSeg, a Python-implemented tool.[35] This applies a novel convolutional neural network-based approach that directly segments WM tracts using a fiber orientation distribution function. As opposed to atlas-based methods, this pipeline does not assume a common anatomy between subjects and therefore relies on each individual's anatomical structure. For every subject, we obtained segmentation of 21 WM tracts of interest based on previous evidence: bilateral uncinate, bilateral inferior longitudinal fascicle, bilateral cingulum, bilateral arcuate fascicle, and bilateral superior longitudinal fascicle divided into three bundles and the corpus callosum divided into seven sections (rostrum, genu, rostral body, anterior midbody, posterior midbody, isthmus, and splenium). Figure 1 is a schematic representation of each tract segmented. Moreover, each tract obtained was divided into 100 segments. Thus, for each position along all tracts, we extracted measures of WM integrity, including fractional anisotropy (FA), as well as mean diffusivity, radial diffusivity (RD), and axial diffusivity.

Further details regarding the TractSeg toolbox can be found in Wasserthal et al.[35] or in the openly available repository: https://github.com/MIC-DKFZ/TractSeg. Out of the total sample, 46 controls, 17 asymptomatic, three prodromal, and five symptomatic *MAPT* carriers were not included in the WM analyses because they did not have a diffusion scan or the data extraction process failed.

2.5 | Functional connectivity analysis

2.5.1 | Preprocessing

T1 scans and fMRI resting-state time series for all participants were preprocessed using fMRIprep 21.0.1 27, an automated Nipype-based preprocessing pipeline for fMRI data implemented in Python, which uses tools from software packages including FSL, ANTs, FreeSurfer, and AFNI.[36] Briefly, the pipeline included bias field correction, skull stripping, brain tissue segmentation, slice time correction, correction for head motion parameters, co-registration to corresponding structural image, and non-linear spatial normalisation to MNI space. Further details on anatomical and functional data preprocessing can be found in Supplementary Methods.

To remove physiological and other sources of noise from the fMRI time series, fMRI confounds generated with fMRIprep were loaded using the Python package load_confound (version 0.6.4.). Six motion parameters, signals estimated from CSF and WM, their derivatives, quadratic terms, and squares of derivatives were regressed out from functional data separately for each run. The rs-fMRI data from each subject was smoothed with a full width at half maximum 6 mm Gaussian kernel and temporally bandpass filtered in the 0.01 to 0.1 Hz frequency range. Resting-state time series with a mean framewise head displacement of more than 0.5 were excluded, as was done in previous work with similar patient populations.

2.5.2 | Parcellating and data extraction

Resting-state time series were spatially parcellated according to the Schaefer atlas (400 parcels across seven functional networks).[37] The Schaefer atlas was chosen for its basis in resting-state functional networks. Using the nilearn connectome Python package, after standardising the time series, we computed each subject's correlation matrix applying the Ledoit-Wolf estimator to adjust for the small number of volumes used and ensure matrix stability for downstream analyses. We then used the bct package implemented in Python to

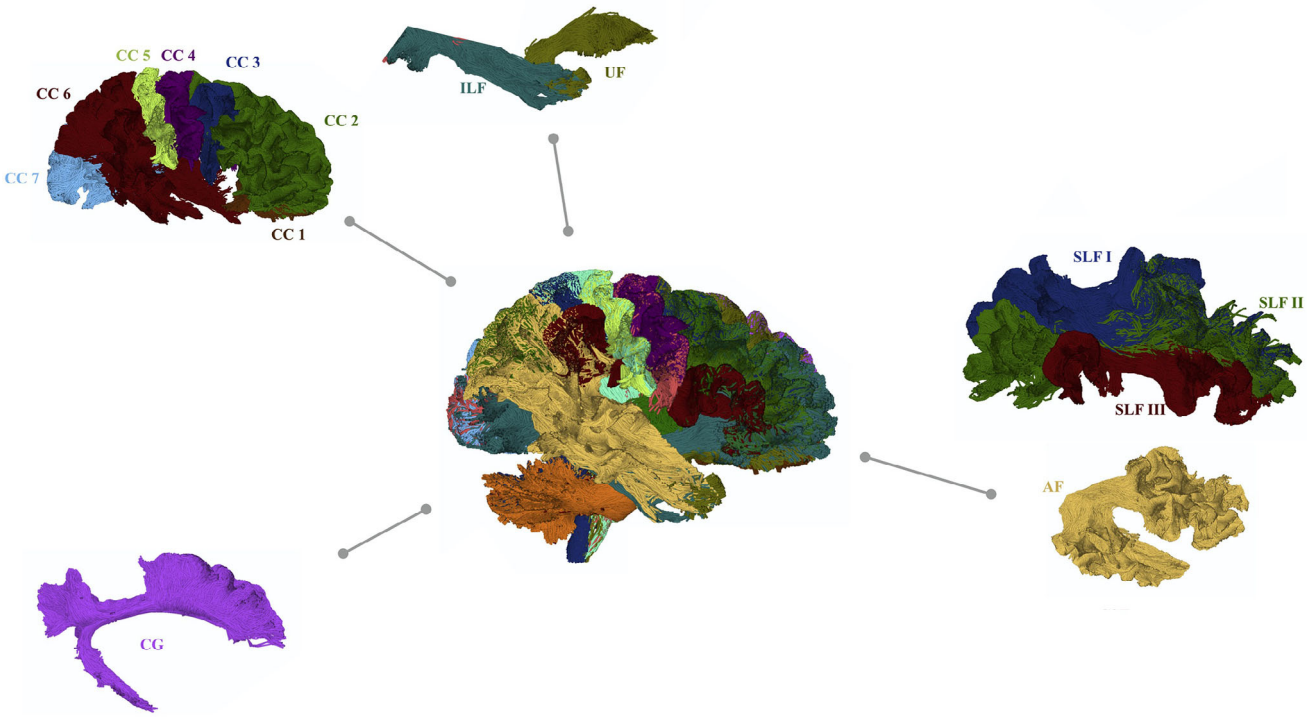

FIGURE 1 Tracts segmented and extracted using the automated TractSeg tool. For tracts existing in the left and right hemispheres, only the right one is shown. Adjusted from Wasserthal et al.[35] AF, arcuate fascicle; CC, corpus callosum (rostrum [CC 1], genu [CC 2], rostral body [CC 3], anterior midbody [CC 4], posterior midbody [CC 5], isthmus [CC 6], splenium [CC 7]); CG, cingulum; ILF, inferior longitudinal fascicle; SLF, superior longitudinal fascicle (I, II, III); UF, uncinate fascicle.

apply a proportional threshold, retaining only the top 17% of strongest connections (by absolute value) in each functional connectivity matrix. The thresholded matrices were then binarised, creating binary masks of the strongest connections. These binary masks were used to filter each corresponding correlation matrix, isolating only the strongest connections for further analysis.

For each parcel of the Schaefer atlas from the binarised and filtered matrices, we extracted four graph theory metrics: two relating to the extent of connections of the parcel and two relating to graph organisational principles. First, degree and strength quantify the number and strength of connections a node (parcel in this case) has. Second, eigenvector centrality considers the centrality and number of connections of a node, while the clustering coefficient corresponds to how much of the network clusters together. These four graph metrics enabled us to assess both local and global properties, offering deeper insights into the structural and functional changes with the different resting-state networks.

Moreover, we extracted macroscale connectivity gradients by applying generalised Canonical Correlation Analysis (gCCA) to all our subjects' time series using the Python-implemented package mvlearn (https://mvlearn.github.io/references/embed.html#generalized-canonical-correlation-analysis-gcca), as was done in previous work.[17,38] This decomposes the functional connectome into primary components, referred to as gradients, with each gradient explaining different levels of variance in connectivity. These gradients discriminate across levels of the cortical hierarchy (i.e., sensory processing vs higher-order cognition), whereas region-specific values along the gradient, referred to as embedding values, reflect the similarity in connectivity along the sensory-transmodal axis. Further details on the connectome gradient mapping specific pipeline can be found in Supplementary Methods.

2.5.3 | Statistical analyses

We compared cortical thickness values between each *MAPT* carrier group and controls using separate general linear models per cortical vertex. These models were adjusted for participants' age, sex, education, total intracranial volume, and site of data acquisition. Pointwise false positives were controlled for with false discovery rate to account for the 327,684 vertices, and cluster-level multiple comparisons were controlled for with random-field theory, applying a vertex-wise cluster threshold of 0.01. Moreover, as the same control group was used in the three models, we corrected the p value threshold using Bonferroni ($0.05/3 = p < 0.016$). We thus identified regions that showed significant reductions of GM thickness in each group compared to controls. We calculated effect sizes for each region using Cohen's d.

WM tract integrity metrics, graph metrics, and connectivity gradient embedding values were compared between each *MAPT* carrier group and controls using linear mixed-effects models. In each model, the metrics were the dependent variables, while network/tract, group, age, and sex were the fixed effects. Site of acquisition, subject, and

parcel/position were included as random effects. We investigated the Network/Tract x Group interaction effect to determine which networks or tracts showed significant differences in each group compared to controls. *P* values were corrected for multiple comparisons using Benjamini and Hochberg for both the number of contrasts and number of networks/tracts.

Statistical analyses were performed using R version 4.3.3.

3 | RESULTS

3.1 | Participant groups

Carriers in the asymptomatic group were significantly younger than controls ($p = 0.003$), while carriers in the symptomatic group were significantly older than controls ($p = 0.0001$). There were no significant differences between any carrier group and controls for years in education or sex distribution ($p > 0.05$). Symptomatic patients scored significantly worse compared to controls on tests spanning visual and verbal memory, processing speed, naming, semantic associations, verbal fluency, executive function, and social cognition. Asymptomatic and prodromal groups showed no significant neuropsychological test score differences compared to controls, apart from better performances in asymptomatic carriers for the Trail Making Test B time ($p = 0.03$) and in prodromal carriers for verbal fluency letter S ($p = 0.04$). Group averages, standard deviations, and *p* values compared to controls are ed in Table 1.

3.2 | Cortical thickness

In asymptomatic carriers, cortical thickness showed sparse areas of thinning in the left anterior cingulate gyrus, with low effect size. In carriers in the prodromal phase, cortical thinning was apparent in the left cingulate and left temporal pole, with medium effect size. Finally, in symptomatic carriers, cortical thinning affected bilateral temporal lobes, both lateral and mesial, left cingulate, as well as bilateral frontal lobes, with high effect sizes. Figure 2 illustrates these results on the cortical surface, and details of the statistical results are reported in Table S3.

3.3 | WM connectivity

No WM tracts showed alterations (in any metric) compared to controls in asymptomatic *MAPT* carriers. However, in prodromal carriers, reduced FA was identified in the rostrum of the corpus callosum, bilateral uncinate fasciculus, and left cingulum compared to controls, as well as increased RD in the left uncinate. In symptomatic *MAPT* carriers, reduced integrity as measured across several metrics was found in the anterior (rostrum, genu, rostral body, anterior midbody) and splenium of the corpus callosum, as well as bilateral uncinate fasciculus, bilateral inferior longitudinal fasciculus, and left cingulum. Figure 3 shows a summary of the results (panel A) as well as the average FA and RD values for each group along the tracts that showed early changes (panel B). The results of the model are presented in Table S4.

3.4 | Functional connectivity

Asymptomatic *MAPT* carriers showed significant differences in eigenvector, degree, and strength, which decreased in the salience ($p < 0.02$) and increased in the visual ($p < 0.0002$) network compared to controls. In prodromal carriers, this pattern was maintained (apart from visual network strength, which did not show significant differences), with further decreases within the salience network. Prodromal carriers also showed the addition of eigenvector reductions in frontoparietal ($p = 0.001$) and increases in sensorimotor ($p = 0.002$) networks, as well as increases in default-mode degree ($p < 0.0001$). There were no significant differences in clustering coefficient for any network in asymptomatic and prodromal carriers ($p > 0.05$). In the symptomatic group, several networks showed reductions across different graph metrics. Figure 4 shows a summary of the results (panel A) as well as the mean values of each metric for each group within the visual and salience networks (panel B). The results of the model are presented in Table S5.

The principal gradient anchored sensorimotor areas at its positive extreme and default mode at its negative extreme, with a gradual transition from sensory to transmodal association networks similar to what was reported in previous work. Along the secondary gradient, the visual network occupied the negative extreme, while areas from the salience populated the positive end of this gradient. Figure 5 illustrates these gradients. These same gradients were reported previously using the same method and a similar population of patients with FTD.[17] Brain regions with the highest or lowest embedding values are at the extremes of the axis, contributing most to the latent component and having the most differentiated functional connectivity. Regions with similar embedding values have similar connectivity patterns, and those near the center (embedding value around 0) contribute less to the latent component.

Principal and secondary gradients revealed some significant differences within middle networks of the gradients in asymptomatic and prodromal groups compared to controls, but not within extreme-end networks. Both the principal and secondary gradients showed widespread differences in various networks in symptomatic *MAPT* carriers. Figure 6 presents the embedding values on the cortical surface for each *MAPT* group for each gradient. The results of the model are presented in Table S6.

4 | DISCUSSION

4.1 | Damage across different disease stages

Aligning with previous research, we found minimal GM reductions at early stages, limited to the left anterior cingulate cortex in asymptomatic carriers and left temporal pole in prodromal carriers.[25,29,39–43] Additionally, asymptomatic carriers showed no evidence of compro-

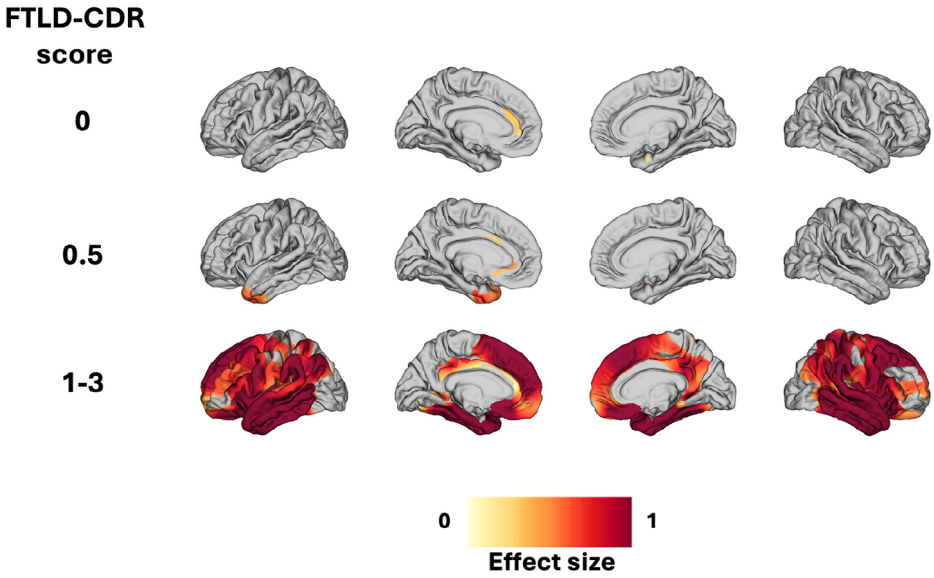

FIGURE 2 Cortical thickness effect sizes (Cohen's *d*) for each microtubule-associated protein tau carrier group compared to controls. FTLD-CDR score,A. Clinical Dementia Rating plus National Alzheimer's Coordinating Center Behavioural and Language domains global score.

mised diffusion in WM tracts, even when using our along-the-tract approach, which allows for the detection of localised changes within specific segments of the tracts. These results show that sparse GM atrophy precedes WM damage in the early disease stages.

Prodromal carriers showed reduced FA in the anterior corpus callosum (rostrum), bilateral uncinate fascicles, and left cingulum, alongside increased radial diffusivity in the left uncinate fascicle. These tracts are located near atrophic regions in the temporal lobes and anterior cingulate, highlighting the synergy between GM and WM changes. Notably, uncinate fascicles have been implicated in studies on presymptomatic *MAPT* carriers.[39,44,45] These structural changes occur in regions and tracts related to early cognitive symptoms in *MAPT* carriers: anomia, semantic and episodic memory impairments.[46–49] Our results show WM integrity becomes affected only in prodromal carriers, when subtle clinical changes may be present but insufficient for a diagnosis.[44,45,50,51] A recent study found WM changes in asymptomatic carriers; however, these results were based on a small sample and were uncorrected for multiple comparisons.[52] Moreover, although some previous work suggested that mean diffusivity was sensitive to early changes in *MAPT* mutation carriers,[51] our findings align with research highlighting the greater sensitivity of FA for detecting such early alterations.[52]

Our results in prodromal carriers support the hypothesis that tau pathology may progress via WM tracts,[53] where tau pathology propagates in a "prion-like" manner along connected networks.[18,54] *Post mortem* studies in *MAPT* mutation carriers[55] and animal models expressing mutant tau[56] confirm early WM degeneration as a key pathological feature. Interestingly, radial diffusivity changes in the left uncinate fascicle were notable in prodromal carriers in our study and showed significant increases in more tracts compared to axial or mean diffusivity in symptomatic carriers, possibly suggesting that myelin is particularly vulnerable to tau pathology. These findings align with studies showing early WM alterations, progressing to disorganised myelinated fiber arrangements with enlarged interaxonal spaces in later stages.[57,58] Our results suggest myelin disruption as a critical element in the progression to bvFTD in *MAPT* mutation carriers.

Contrasting with the onset of structural connectivity changes in the prodromal stage, functional connectivity alterations were evident in asymptomatic carriers ($n = 47$), with graph metrics found to be decreased in the salience but increased in the visual network. Functional connectivity changes in *MAPT* carriers, particularly in the salience network and anterior cingulate cortex, have been reported before.[28,39,59] PET studies further highlight early functional alterations in the anterior cingulate and insula regions,[25–27] which are found *post mortem* to be most affected by tau aggregation in *MAPT*-associated FTD.[60] Moreover, these regions align with clinical symptoms of bvFTD, involving executive dysfunction, apathy, and social cognition deficits. As graph metric alterations correlate with synaptic density, early functional connectivity changes likely reflect synaptic disruptions.[61] Synaptic loss accounts for functional connectivity reductions not explained by atrophy, suggesting these changes may precede myelin and axonal damage as well as GM atrophy. Together, these findings point toward a progression from early synaptic dysfunction to structural degeneration in *MAPT*-related neurodegeneration, though this warrants validation in a longitudinal sample.

4.2 | Neural compensation

Our study is the first to identify functional connectivity changes in visual network in presymptomatic *MAPT* carriers, despite the preserved structural integrity of the occipital lobe even in later disease stages. This may reflect connectomal diaschisis, where a "lesion" induces distal connectivity changes, either increased or decreased.[62]

(A)

	MAPT 0	MAPT 0.5	MAPT 1-3
FA		Corpus callosum rostrum * Bilateral uncinate * Left cingulum *	Anterior corpus callosum (rostrum-midbody) * * & splenium * * Bilateral uncinate * * Left cingulum * Bilateral inferior longitudinal * Left superior longitudinal III *
MD			Anterior corpus callosum (rostrum-rostral body) * * & splenium * * Bilateral uncinate * * Bilateral inferior longitudinal * * Left superior longitudinal III *
RD		Left uncinate *	Corpus callosum (rostrum-rostral body) * * & splenium * * Bilateral uncinate * * Left cingulum * Inferior longitudinal * * Right superior longitudinal II * Bilateral superior longitudinal III *
AD			Bilateral inferior longitudinal * Bilateral uncinate * *

(B)

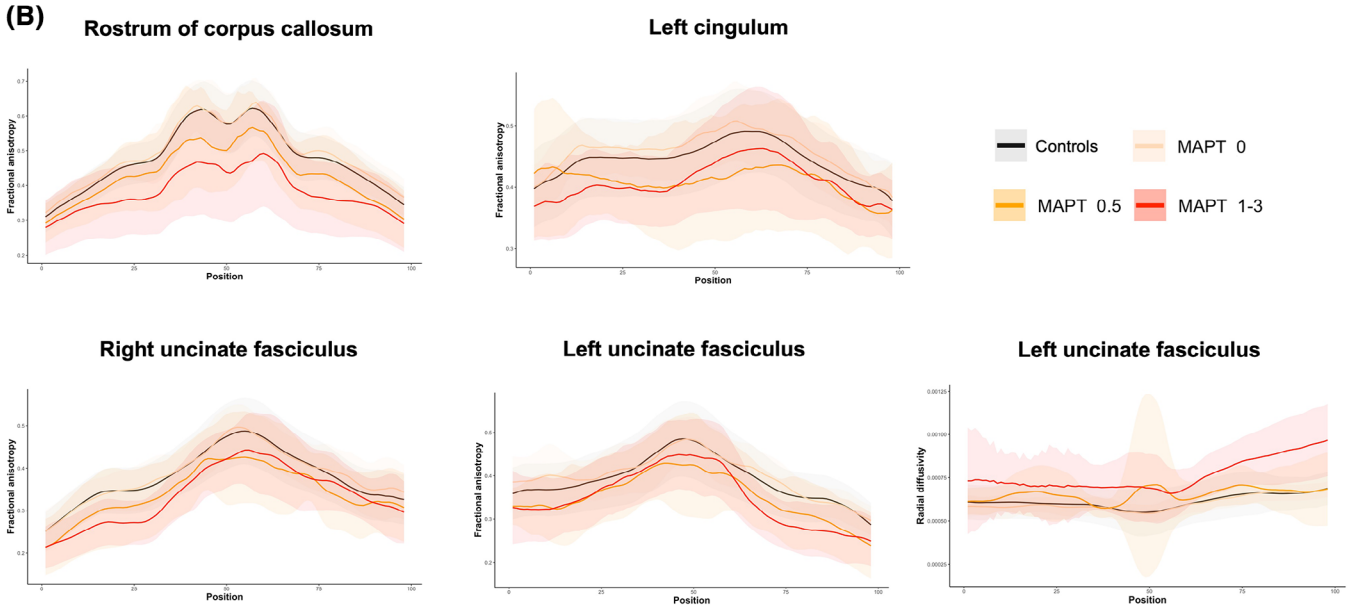

FIGURE 3 A. Summary of tracts showing significantly different diffusion metrics in each microtubule associated protein tau (*MAPT*) carrier group compared to controls, $^{*}p < 0.05$, $^{**}p < 0.005$. FA, fractional anisotropy; MD, mean diffusivity; RD, radial diffusivity; AD, axial diffusivity. B. Adjusted mean fractional anisotropy and radial diffusivity values from mixed model for each group, with shaded standard deviation, along tracts showing significant early changes in MAPT prodromal carriers compared to controls.

Consistent with this concept, visual network exhibited connectivity changes opposite to those observed in salience network, which aligns with expected pathology-driven alterations. In the same vein, enhanced metabolic activity in asymptomatic *MAPT* carriers, which diminishes in symptomatic stages, has been reported.[26] Similar visual network alterations have been observed in patients with sporadic bvFTD and primary progressive aphasia using functional connectome gradient mapping.[17] Such changes may arise from overexcitation due to reduced inhibitory control from affected networks, such as the salience network.[11,13,63–65] Alternatively, they may reflect compensatory mechanisms in response to pathology.[17] Despite early functional disruptions, *MAPT* carriers remained clinically asymptomatic, as highlighted by finding no differences between their cognitive test scores and those of controls (or, if so, better performances), supporting the concepts of neurodevelopmental resilience in genetic FTD[66] and compensatory hyperconnectivity preserving cognitive function in early disease stages.[28] These findings suggest that pathology-induced disruptions in certain networks may drive increased visual network connectivity, highlighting the interplay between resilience and vulnerability in early *MAPT*-related neurodegeneration.

The extent to which *MAPT* mutations cause neurodevelopmental differences in human carriers remains unclear. However, it is well established that tau expression changes dynamically during neurodevelopment, with isoform expression varying across neurodevelopmental and neurodegenerative stages.[67] Decades ago, it was suggested that abnormal tau phosphorylation in neurodegenerative diseases, such as Alzheimer's, may result from the reactivation of pathways involved in tau phosphorylation during brain development.[68] The functional connectivity differences observed in our study may reflect altered "wiring" of the brain in *MAPT* mutation carriers from development, potentially representing compensatory mechanisms that delay pathological tau aggregation during early neurodevelopment.[66] Studying carriers at a young age could help distinguish between changes stemming from neurodevelopmental processes and those related to early neurodegeneration, providing crucial insights for developing intervention strategies for *MAPT* mutation carriers.

(A)

	MAPT 0	MAPT 0.5	MAPT 1-3
Strength	Salience ↓ Visual ↑	Salience ↓	Salience ↓ Sensorimotor ↓
Degree	Salience ↓ Visual ↑	Default-mode ↑ Salience ↓ Visual ↑	frontoparietal ↓ Default-mode ↓ Salience ↓ Sensorimotor ↓ Visual ↓
Eigenvector	Salience ↓ Visual ↑	Salience ↓ Visual ↑ Frontoparietal ↓ Sensorimotor ↑	Salience ↓ Visual ↓ Frontoparietal ↓ Sensorimotor ↓ Dorsal attentional ↓ Default-mode ↓
Clustering			Sensorimotor ↓ Salience ↓

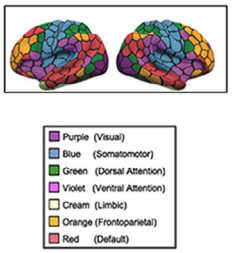

(B)

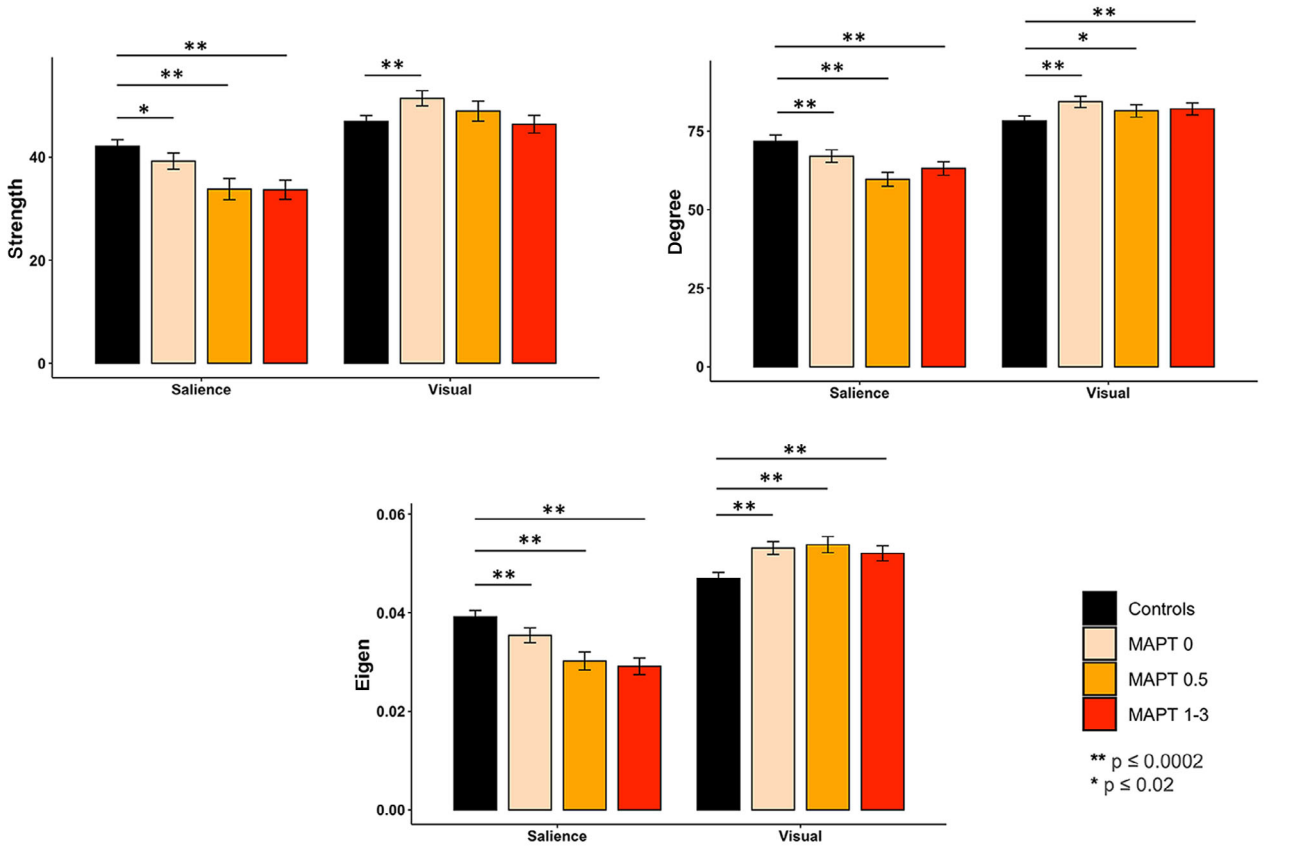

FIGURE 4 A. Summary of networks showing significant different graph metrics in each microtubule associated protein tau (*MAPT*) carrier group compared to controls, with the direction of change depicted by an arrow. B. Adjusted means and standard errors from mixed model for each group and for different graph metrics within salience and visual networks which showed early changes compared to controls.

4.3 | Complementary measures of functional connectivity

Our analysis showed focal functional connectivity changes from the asymptomatic stage, while global disruptions were only evident in symptomatic stages. Clustering and macroscale gradients remained intact in asymptomatic and prodromal carriers. Specifically, no major differences were observed in the principal or secondary gradients, with preserved organisation of extreme-end networks (sensorimotor and default mode for the principal gradient, salience and visual for the secondary gradient). This contrasts with findings in symptomatic FTD[17] and aligns with reports of within-network changes and intact

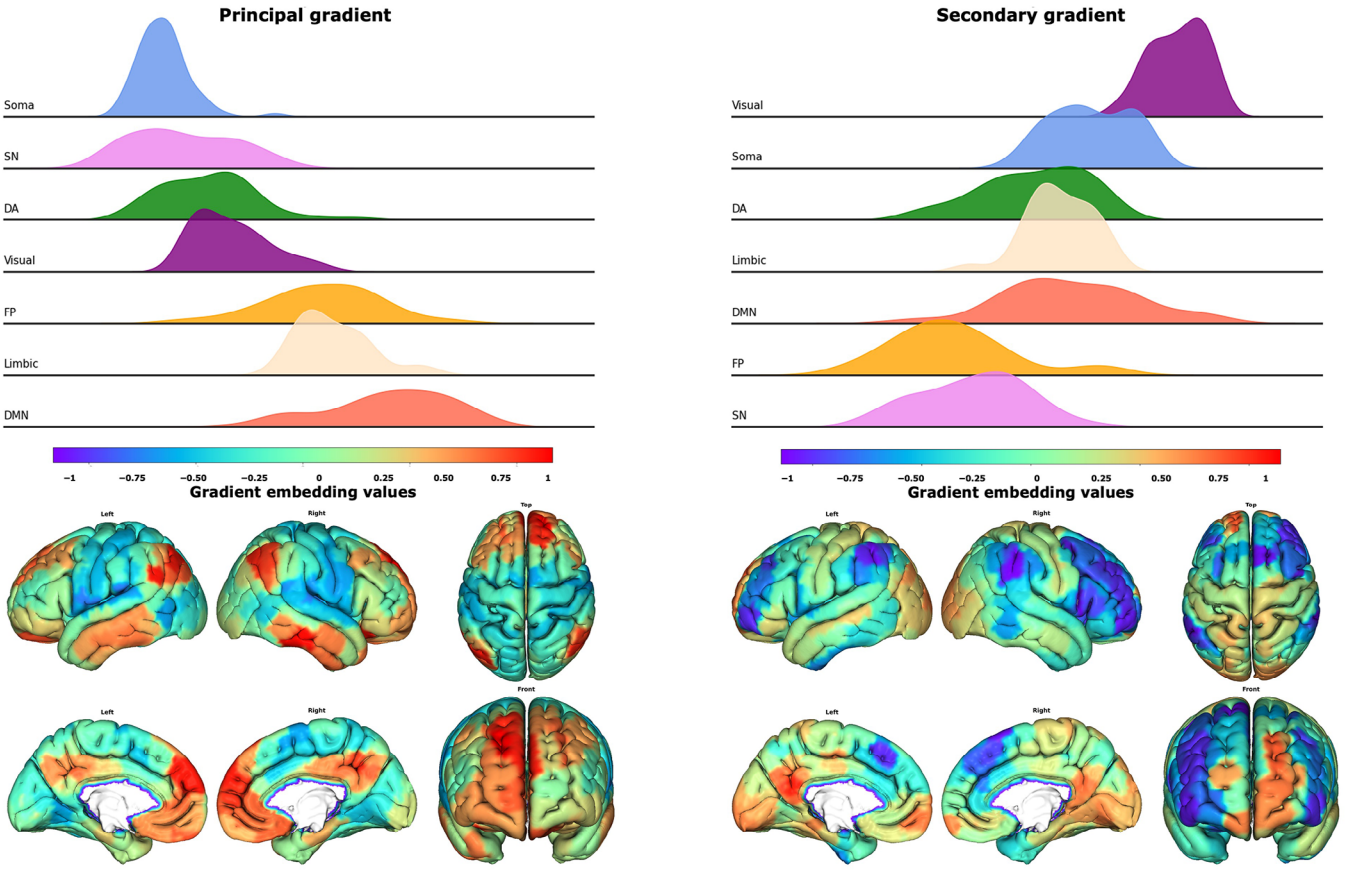

FIGURE 5 Distribution of principal and secondary gradient embedding values for each network in controls and projected on cortical surface.

global organisation in presymptomatic carriers.[69] These results suggest global connectivity, crucial for cognitive resilience, is preserved at early stages, with structural and functional disruptions becoming widespread only at symptom onset.[69,70] Again, this aligns with our findings of preserved cognitive function in asymptomatic and prodromal *MAPT* mutation carrier groups.

4.4 | Theoretical progression model

Our findings suggest a pathophysiological progression model for *MAPT* mutation carriers that begins with focal tau pathology targeting neurons within functional network hubs (anterior cingulate cortex). This leads to sparse early GM atrophy. Early functional connectivity network, related to the targeted neurons (salience network) but also those that are not (visual network), are either triggered by this pathology or serve a (compensatory) function different from that of controls, possibly since neurodevelopment stages. Network disruptions likely encourage the propagation of pathology via initially intact axonal pathways, causing demyelination and diffuse structural connectivity changes in regions connected to affected hubs. These stages align with the hypothesis of tau spreading along axonal connections,[71] causing functional network disruptions before widespread atrophy occurs. Very recent work in Alzheimer's disease suggests that pathological protein deposition of amyloid beta can induce hyperconnectivity between tau epicenters and posterior brain regions vulnerable to tau accumulation, with this increased connectivity mediating faster tau spreading.[72] This again highlights that hyperconnectivity precedes neocortical tau propagation while being instrumental in its progression.

We propose a theoretical model of biomarker evolution in *MAPT* mutation carriers (Figure 7), where functional dysconnectivity emerges as an initial disease indicator, followed by structural degeneration as the disease advances. Structural connectivity disruptions become widespread in later stages, coinciding with global functional alterations. Our framework aligns with prior hypotheses,[73] incorporating multimodal data from the same cohort and offering robust evidence for the dynamic progression of *MAPT*-related neurodegeneration. Early focal functional changes, potentially reversible, may serve as biomarkers for monitoring treatment efficacy, while later structural alterations signify irreversible damage. Validating these biomarkers is crucial for enhancing patient stratification and evaluating disease-modifying therapies in clinical trials.

4.5 | Strengths and limitations

Our study benefited from multimodal imaging to evaluate structural and functional connectivity in conjunction, a rarity in presymptomatic

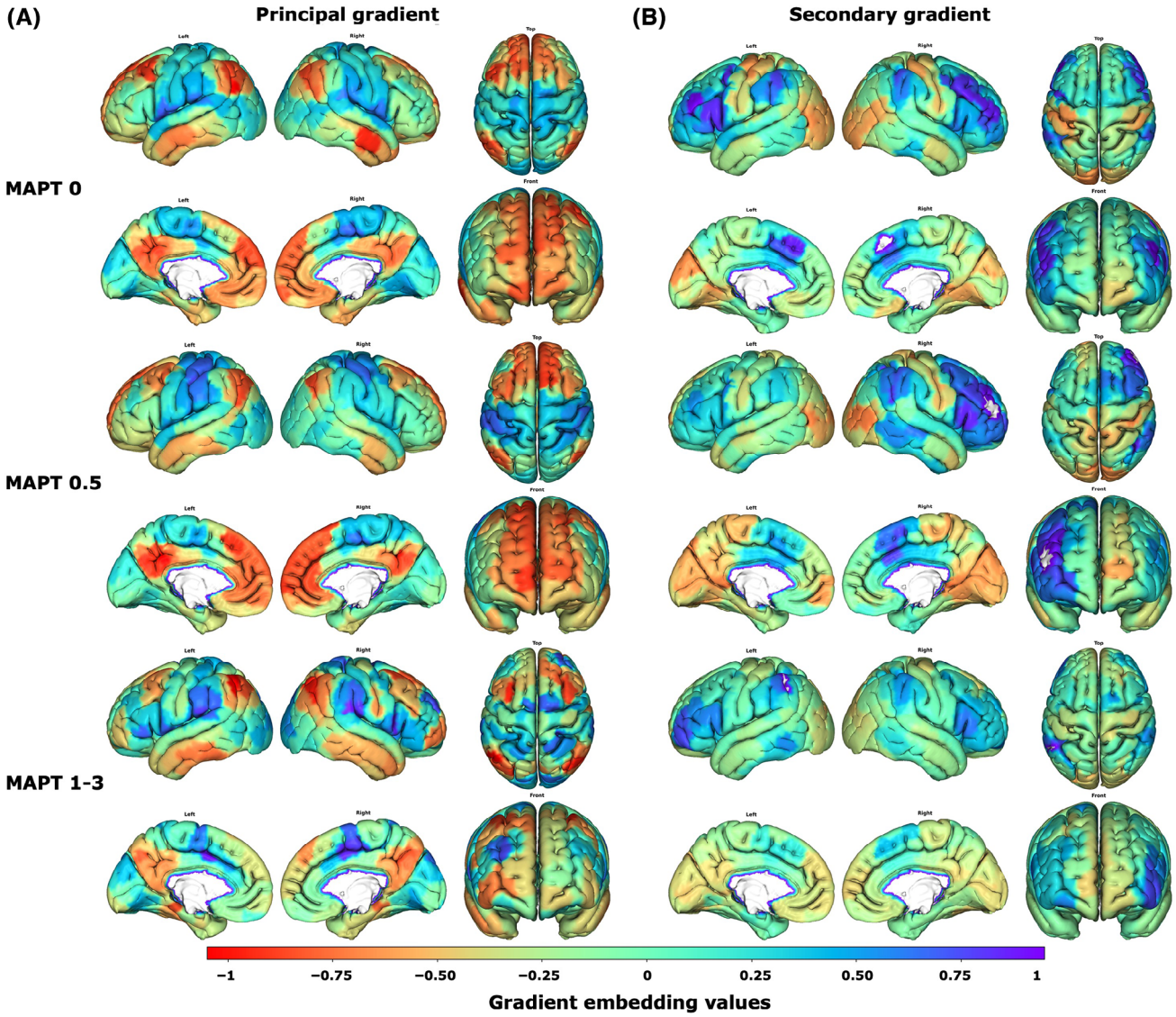

FIGURE 6 Principal and secondary gradient embedding values projected on cortical surface for each microtubule associated protein tau (*MAPT*) carrier group.

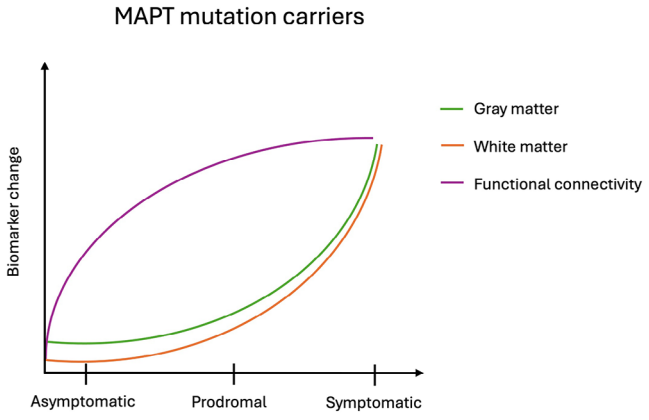

FIGURE 7 Theoretical model of gray matter, white matter, and functional connectivity neuroimaging biomarker evolution in microtubule-associated protein tau-mutation carriers.

FTD research. Large sample sizes enabled precise subgrouping while avoiding underpowered groups, though the prodromal carrier group remained modest. Moreover, the large control group enabled a more accurate assessment of potential demographic influences, such as sex and age, which were unevenly distributed across the different carrier groups and were therefore included as covariates in our statistical models. Notably, we observed contrasting sex ratios: asymptomatic and prodromal carriers were predominantly female, whereas symptomatic carriers were more often male. This discrepancy was likely influenced by societal factors, as women are more frequently primary caregivers and tend to remain in this role for longer, a pattern that is well documented in dementia research.[74]

The study's quasi-longitudinal design provides valuable insights but cannot replace true longitudinal studies, which are essential to validate our results and refine our theoretical biomarker evolution model. Further, we did not analyse mutation-specific differences, which

are known to influence atrophy patterns.[75] Additionally, though both structural and functional neuroimaging modalities were included, tractography and connectomics are completely different methodologies with disparate underlying priors. Therefore, our findings cannot be directly compared. Employing multivariate multimodal methods would enhance the integration and interpretation of these findings.

5 | CONCLUSION

MRI biomarkers, being non-invasive, cost-effective, and suitable for longitudinal studies, hold promise for tracking or predicting disease progression and guiding therapeutic strategies. This study highlights functional connectivity changes as an early biomarker and structural changes as indicators of advanced stages. By interpreting these findings balancing pathology and compensation, we propose a model of biomarker evolution in *MAPT*-related neurodegeneration. Understanding these dynamics, whether specific to tau pathology or shared across proteinopathies, could aid in developing early interventions to preserve compensation and slow progression. In conclusion, our results highlight the relevance of investigating GM and WM structure alongside functional connectivity in genetic FTD, particularly in presymptomatic stages. Although not directly translatable to clinical use yet, these findings lay essential groundwork for future biomarker development and patient stratification.

AFFILIATIONS

[1]Paris Brain Institute, Sorbonne Université, INSERM U1127, Hôpital Pitié-Salpêtrière, Paris, France

[2]Dementia Research Centre, Department of Neurodegenerative Disease, UCL Queen Square Institute of Neurology, London, UK

[3]Centre de référence des démences rares ou précoces, IM2A, Département de Neurologie, AP-HP - Hôpital Pitié-Salpêtrière, Paris, France

[4]Department of Neurology, Erasmus Medical Centre, Rotterdam, Netherlands

[5]Alzheimer's Disease and Other Cognitive Disorders Unit, Neurology Service, Hospital Clínic, Institut d'Investigacións Biomèdiques August Pi I Sunyer, University, Barcelona, Spain

[6]Clinique Interdisciplinaire de Mémoire, Département des Sciences Neurologiques, CHU de Québec, and Faculté de Médecine, Université Laval, Quebec, Canada

[7]Department of Neurobiology, Care Sciences and Society, Center for Alzheimer Research, Division of Neurogeriatrics, Bioclinicum, Karolinska Institutet, Solna, Sweden

[8]Unit for Hereditary Dementias, Theme Inflammation and Aging, Karolinska University Hospital, Solna, Sweden

[9]Fondazione Ca' Granda, IRCCS Ospedale Policlinico, Milan, Italy

[10]University of Milan, Centro Dino Ferrari, Milan, Italy

[11]Laboratory for Cognitive Neurology, Department of Neurosciences, KU Leuven, Leuven, Belgium

[12]Neurology Service, University Hospitals Leuven, Leuven, Belgium

[13]Leuven Brain Institute, KU Leuven, Leuven, Belgium

[14]Faculty of Medicine, University of Lisbon, Lisbon, Portugal

[15]Fondazione IRCCS Istituto Neurologico Carlo Besta, Milano, Italy

[16]University Hospital of Coimbra (HUC), Neurology Service, Faculty of Medicine, University of Coimbra, Coimbra, Portugal

[17]Center for Neuroscience and Cell Biology, Faculty of Medicine, University of Coimbra, Coimbra, Portugal

[18]Division of Psychology Communication and Human Neuroscience, Wolfson Molecular Imaging Centre, University of Manchester, Manchester, UK

[19]Department of Nuclear Medicine, Center for Translational Neuro- and Behavioral Sciences, University Medicine Essen, Essen, Germany

[20]Department of Geriatric Medicine, Klinikum Hochsauerland, Arnsberg, Germany

[21]Department of Neurology, Ludwig-Maximilians Universität München, Munich, Germany

[22]German Center for Neurodegenerative Diseases (DZNE), Munich, Germany

[23]Munich Cluster of Systems Neurology (SyNergy), Munich, Germany

[24]Department of Neurofarba, University of Florence, Florence, Italy

[25]IRCCS Fondazione Don Carlo Gnocchi, Florence, Italy

[26]Department of Neurology, University of Ulm, Ulm, Germany

[27]Lille Neuroscience & Cognition U1172, University of Lille, Inserm, CHU Lille, France

[28]Department of Psychiatry, McGill University Health Centre, McGill University, Montreal, Québec, Canada

[29]McConnell Brain Imaging Centre, Montreal Neurological Institute, McGill University, Montreal, Québec, Canada

[30]Nuffield Department of Clinical Neurosciences, Medical Sciences Division, University of Oxford, Oxford, UK

[31]Department of Brain Sciences, Imperial College London, London, UK

[32]Department of Clinical Neurological Sciences, University of Western Ontario, London, Ontario, Canada

[33]Tanz Centre for Research in Neurodegenerative Diseases, University of Toronto, Toronto, Ontario, Canada

[34]Sunnybrook Health Sciences Centre, Sunnybrook Research Institute, University of Toronto, Toronto, Canada

[35]MRC Cognition and Brain Sciences Unit, University of Cambridge, Cambridge, UK

[36]Department of Neurodegenerative Diseases, Hertie-Institute for Clinical Brain Research and Center of Neurology, University of Tübingen, Tübingen, Germany

[37]Cognitive Disorders Unit, Department of Neurology, Hospital Universitario Donostia, San Sebastian, Spain

[38]Biogipuzkoa Health Research Institute, Neurosciences Area, Group of Neurodegenerative Diseases, San Sebastian, Spain

[39]Center for Biomedical Research in Neurodegenerative Disease (CIBERNED), Carlos III Health Institute, Madrid, Spain

[40]Department of Clinical and Experimental Sciences, University of Brescia, Brescia, Italy

[41]Molecular Markers Laboratory, IRCCS Istituto Centro San Giovanni di Dio Fatebenefratelli, Brescia, Italy

CONSORTIUM AUTHOR LIST

Rhian Convery; Martina Bocchetta; David Cash; Sophie Goldsmith; Kiran Samra; David L. Thomas; Thomas Cope; Maura Malpetti; Antonella Alberici; Enrico Premi; Roberto Gasparotti; Emanuele Buratti; Valentina Cantoni; Andrea Arighi; Chiara Fenoglio; Vittoria Borracci; Maria Serpente; Tiziana Carandini; Emanuela Rotondo; Giacomina Rossi; Giorgio Giaccone; Giuseppe Di Fede; Paola Caroppo; Sara Prioni; Veronica Redaelli; David Tang-Wai; Ekaterina Rogaeva;

Johanna Krüger; Miguel Castelo-Branco; Morris Freedman; Ron Keren; Sandra Black; Sara Mitchell; Christen Shoesmith; Robart Bartha; Rosa Rademakers; Jackie Poos; Janne M. Papma; Lucia Giannini; Liset de Boer; Julie de Houwer; Rick van Minkelen; Yolande Pijnenburg; Benedetta Nacmias; Camilla Ferrari; Cristina Polito; Gemma Lombardi; Valentina Bessi; Enrico Fainardi; Stefano Chiti; Mattias Nilsson; Henrik Viklund; Melissa Taheri Rydell; Vesna Jelic; Abbe Ullgren; Elena Rodriguez-Vieitez; Tobias Langheinrich; Albert Lladó; Anna Antonell; Jaume Olives; Mircea Balasa; Nuria Bargalló; Sergi Borrego-Ecija; Ana Verdelho; Carolina Maruta; Tiago Costa-Coelho; Gabriel Miltenberger; Frederico Simões do Couto; Alazne Gabilondo; Ioana Croitoru; Mikel Tainta; Myriam Barandiaran; Patricia Alves; Benjamin Bender; David Mengel; Lisa Graf; Annick Vogels; Mathieu Vandenbulcke; Philip Van Damme; Rose Bruffaerts; Koen Poesen; Pedro Rosa-Neto; Maxime Montembault; Ninon Burgos; Daisy Rinaldi; Catharina Prix; Elisabeth Wlasich; Olivia Wagemann; Sonja Schönecker; Alexander Maximilian Bernhardt; Anna Stockbauer; Jolina Lombardi; Sarah Anderl-Straub; Adeline Rollin; Gregory Kuchcinski; Vincent Deramecourt; João Durães; Marisa Lima; Maria João Leitão; Maria Rosario Almeida; Miguel Tábuas-Pereira; Sónia Afonso; João Lemos

ACKNOWLEDGMENTS

The authors thank the research participants and their families for their contribution to the study.

R.S.-V. was funded at the Hospital Clinic de Barcelona by the Instituto de Salud Carlos III, Spain (grant code PI20/00448 to RSV) and Fundació Marató TV3, Spain (grant code 20143810 to RSV). R.L. is supported by the Canadian Institutes of Health Research and the Chaire de Recherche sur les Aphasies Primaires Progressives Fondation Famille Lemaire. C.G. is supported by the Swedish Frontotemporal Dementia Initiative Schörling Foundation; Vetenskapsrådet (Swedish Research Council) JPND Prefrontals, 2015-02926, 2018-02754, and JPND-GENFI-PROX 2019-02248; Swedish Alzheimer Foundation, ALF-project Region Stockholm, Karolinska Institutet Doctoral Funding, KI Strat-Neuro, Swedish Dementia Foundation, and Swedish Brain-Foundation. This work was funded by Mady Browaeys Fonds voor Onderzoek naar Frontotemporale Degeneratie. J.L. is funded by the Deutsche Forschungsgemeinschaft (DFG, German Research Foundation) under Germany's Excellence Strategy within the framework of the Munich Cluster for Systems Neurology (EXC 2145 SyNergy – ID 390857198). S.D. receives salary funding from the Fonds de Recherche du Québec—Santé. This research was undertaken thanks in part to funding from the Canada First Research Excellence Fund, awarded to McGill University for the Healthy Brains, Healthy Lives initiative. This work was supported by ANR-PRTS PREV-DemAls, PHRC PREDICT-PGRN and several authors of this publication are members of the European Reference Network for Rare Neurological Diseases—Project ID No 739510. M.M. was, in part, funded by the UK Medical Research Council, the Italian Ministry of Health and the Canadian Institutes of Health Research as part of a Centres of Excellence in Neurodegeneration grant, and also Canadian Institutes of Health Research operating grants (Grant #s: MOP- 371851 and PJT-175242) and funding from the Weston Brain Institute to Mario Masellis. J.B.R. has received funding from the Wellcome Trust (103838; 220258), the Bluefield Project, and is supported by the Cambridge University Centre for Frontotemporal Dementia, the Medical Research Council (MC_UU_00030/14; MR/T033371/1) and the National Institute for Health Research Cambridge Biomedical Research Centre (NIHR203312). For the purpose of open access, the author applied a CC BY public copyright license to any Author Accepted Manuscript version arising from this submission. This work was supported by the JPND grant "GENFI-prox" (by DLR/BMBF to M.S, joint with J.R., JvS, M.O., B.B., and C.G.). F.M. is supported by the Tau Consortium and has received funding from the Carlos III Health Institute (PI19/01637). B.B. is supported by JPND grant "GENFI-prox" (2019-02248). J.D.R. is supported by the Miriam Marks Brain Research UK Senior Fellowship and has received funding from a MRC Clinician Scientist Fellowship (MR/M008525/1) and the NIHR Rare Disease Translational Research Collaboration (BRC149/NS/MH). This work was also supported by the Medical Research Cc UK GENFI grant (MR/M023664/1), the Bluefield Project, and the JPND GENFI-PROX grant (2019-02248).

Arabella Bouzigues is funded by a PhD Fellowship from the Fondation Recherche Alzheimer (FRA) and the Association pour la Recherche sur la SLA (ARSLA). John C. van Swieten, L.C.J., and H.S. are supported by the Dioraphte Foundation grant 09-02-03-00, Association for Frontotemporal Dementias Research Grant 2009, Netherlands Organization for Scientific Research grant HCMI 056-13-018, ZonMw Memorabel (Deltaplan Dementie, project number 733 051 042), ZonMw Onderzoeksprogramma Dementie (YOD-INCLUDED, project no. 10510032120002), EU Joint Programme-Neurodegenerative Disease Research-GENFI-PROX, Alzheimer Nederland, and the Bluefield Project. R.S-V. is supported by Alzheimer's Research UK Clinical Research Training Fellowship (ARUK-CRF2017B-2) and has received funding from Fundació Marató de TV3, Spain (grant no. 20143810). C.G. received funding from EU Joint Programme-Neurodegenerative Disease Research-Prefrontals Vetenskapsrådet Dnr 529-2014-7504, EU Joint Programme-Neurodegenerative Disease Research-GENFI-PROX, Vetenskapsrådet 2019-0224, Vetenskapsrådet 2015-02926, Vetenskapsrådet 2018-02754, the Swedish FTD Inititative-Schörling Foundation, Alzheimer Foundation, Brain Foundation, Dementia Foundation, and Region Stockholm ALF-project. D.G. received support from the EU Joint Programme–Neurodegenerative Disease Research and the Italian Ministry of Health (PreFrontALS) grant 733051042. R.V. has received funding from the Mady Browaeys Fund for Research into Frontotemporal Dementia. J.L. received funding for this work by the Deutsche Forschungsgemeinschaft German Research Foundation under Germany's Excellence Strategy within the framework of the Munich Cluster for Systems Neurology (EXC 2145 SyNergy—ID 390857198). M.O. has received funding from Germany's Federal Ministry of Education and Research (BMBF). E.F. has received funding from a Canadian Institute of Health Research grant 327387. M.M. has received funding from a Canadian Institute of Health Research operating grant and the Weston Brain Institute and Ontario Brain Institute. J.B.R. has received funding from the Wellcome Trust (103838; 220258), the Bluefield Project, and is supported by the Cambridge University Centre for Frontotemporal Dementia, the Medical Research

Council (MC_UU_00030/14; MR/T033371/1) and the National Institute for Health Research Cambridge Biomedical Research Centre (NIHR203312). For the purpose of open access, the author applied a CC BY public copyright license to any Author Accepted Manuscript version arising from this submission. F.M. is supported by the Tau Consortium and has received funding from the Carlos III Health Institute (PI19/01637). J.D.R. is supported by the Bluefield Project and the National Institute for Health and Care Research University College London Hospitals Biomedical Research Centre and has received funding from a MRC Clinician Scientist Fellowship (MR/M008525/1) and a Miriam Marks Brain Research UK Senior Fellowship. R.M. is supported by France Alzheimer, Fondation Recherche Alzheimer, Fondation Philippe Chatrier, and Rosita Gomez association. Several authors of this publication (J.C.V.S., M.S., R.V., A.d.M., M.O., R.V., J.D.R.) are members of the European Reference Network for Rare Neurological Diseases (ERN-RND)–Project ID No. 739510. This work was also supported by the EU Joint Programme—Neurodegenerative Disease Research GENFI-PROX grant (2019-02248; to J.D.R., M.O., B.B., C.G., J.C.V.S., and M.S).

Local ethics committees approved the study at each site, and all participants provided written informed consent. The study was conducted according to the Declaration of Helsinki.

CONFLICT OF INTEREST STATEMENT

The authors declare no conflicts of interest. Author disclosures are available in the Supporting Information.

ORCID

Arabella Bouzigues https://orcid.org/0000-0002-0267-8590

REFERENCES

1. Poorkaj P, Bird TD, Wijsman E, et al. Tau is a candidate gene for chromosome 17 frontotemporal dementia. *Ann Neurol*. 1998;43(6):815-825. doi:10.1002/ana.410430617
2. Moore KM, Nicholas J, Grossman M, et al. Age at symptom onset and death and disease duration in genetic frontotemporal dementia: an international retrospective cohort study. *Lancet Neurol*. 2020;19(2):145-156. doi:10.1016/S1474-4422(19)30394-1
3. Van Swieten J, Spillantini MG. Hereditary frontotemporal dementia caused by tau gene mutations. *Brain Pathol*. 2007;17(1):63-73. doi:10.1111/j.1750-3639.2007.00052.x
4. Woollacott IOC, Rohrer JD. The clinical spectrum of sporadic and familial forms of frontotemporal dementia. *J Neurochem*. 2016;138(S1):6-31. doi:10.1111/jnc.13654
5. Staffaroni AM, Quintana M, Wendelberger B, et al. Temporal order of clinical and biomarker changes in familial frontotemporal dementia. *Nat Med*. 2022;28(10):2194-2206. doi:10.1038/s41591-022-01942-9
6. Seeley WW, Menon V, Schatzberg AF, et al. Dissociable intrinsic connectivity networks for salience processing and executive control. *J Neurosci*. 2007;27(9):2349-2356. doi:10.1523/JNEUROSCI.5587-06.2007
7. Zhou J, Greicius MD, Gennatas ED, et al. Divergent network connectivity changes in behavioural variant frontotemporal dementia and Alzheimer's disease. *Brain*. 2010;133(5):1352-1367. doi:10.1093/brain/awq075
8. Zhou J, Liu S, Ng KK, Wang J. Applications of resting-state functional connectivity to neurodegenerative disease. *Neuroimaging Clin*. 2017;27(4):663-683. doi:10.1016/j.nic.2017.06.007
9. Whitwell JL, Weigand SD, Gunter JL, et al. Trajectories of brain and hippocampal atrophy in FTD with mutations in MAPT or GRN. *Neurology*. 2011;77(4):393-398. doi:10.1212/WNL.0b013e318227047f
10. Borroni B, Grassi M, Premi E, et al. Neuroanatomical correlates of behavioural phenotypes in behavioural variant of frontotemporal dementia. *Behav Brain Res*. 2012;235(2):124-129. doi:10.1016/j.bbr.2012.08.003
11. Farb NAS, Grady CL, Strother S, et al. Abnormal network connectivity in frontotemporal dementia: evidence for prefrontal isolation. *Cortex J Devoted Study Nerv Syst Behav*. 2013;49(7):1856-1873. doi:10.1016/j.cortex.2012.09.008
12. Pievani M, Filippini N, van den Heuvel MP, Cappa SF, Frisoni GB. Brain connectivity in neurodegenerative diseases—from phenotype to proteinopathy. *Nat Rev Neurol*. 2014;10(11):620-633. doi:10.1038/nrneurol.2014.178
13. Agosta F, Sala S, Valsasina P, et al. Brain network connectivity assessed using graph theory in frontotemporal dementia. *Neurology*. 2013;81(2):134-143. doi:10.1212/WNL.0b013e31829a33f8
14. Agosta F, Ferraro PM, Canu E, et al. Differentiation between subtypes of primary progressive aphasia by using cortical thickness and diffusion-tensor MR imaging measures. *Radiology*. 2015;276(1):219-227. doi:10.1148/radiol.15141869
15. Agosta F, Spinelli EG, Basaia S, et al. Functional connectivity from disease epicenters in frontotemporal dementia. *Neurology*. 2023;100(22):e2290-e2303. doi:10.1212/WNL.0000000000207277
16. Brown JA, Deng J, Neuhaus J, et al. Patient-tailored, connectivity-based forecasts of spreading brain atrophy. *Neuron*. 2019;104(5):856-868.e5. doi:10.1016/j.neuron.2019.08.037
17. Bouzigues A, Godefroy V, Le Du V, et al. Disruption of macroscale functional network organisation in patients with frontotemporal dementia. *Mol Psychiatry*. 2025;30(6):2436-2447. doi:10.1038/s41380-024-02847-4
18. Seeley WW, Crawford RK, Zhou J, Miller BL, Greicius MD. Neurodegenerative diseases target large-scale human brain networks. *Neuron*. 2009;62(1):42-52. doi:10.1016/j.neuron.2009.03.024
19. Raj A, Kuceyeski A, Weiner M. A network diffusion model of disease progression in dementia. *Neuron*. 2012;73(6):1204-1215. doi:10.1016/j.neuron.2011.12.040
20. Zhou J, Gennatas ED, Kramer JH, Miller BL, Seeley WW. Predicting regional neurodegeneration from the healthy brain functional connectome. *Neuron*. 2012;73(6):1216-1227. doi:10.1016/j.neuron.2012.03.004
21. Mandelli ML, Vilaplana E, Brown JA, et al. Healthy brain connectivity predicts atrophy progression in non-fluent variant of primary progressive aphasia. *Brain*. 2016;139(10):2778-2791. doi:10.1093/brain/aww195
22. Frost B, Diamond MI. Prion-like mechanisms in neurodegenerative diseases. *Nat Rev Neurosci*. 2010;11(3):155-159. doi:10.1038/nrn2786
23. Liu L, Drouet V, Wu JW, et al. Trans-synaptic spread of tau pathology in vivo. *PLoS One*. 2012;7(2):e31302. doi:10.1371/journal.pone.0031302
24. Dopper EGP, Rombouts SARB, Jiskoot LC, et al. Structural and functional brain connectivity in presymptomatic familial frontotemporal dementia. *Neurology*. 2013;80(9):814-823. doi:10.1212/WNL.0b013e31828407bc
25. Clarke MTM, St-Onge F, Beauregard JM, et al. Early anterior cingulate involvement is seen in presymptomatic MAPT P301L mutation carriers. *Alzheimers Res Ther*. 2021;13(1):42. doi:10.1186/s13195-021-00777-9
26. Liu L, Chu M, Nie B, et al. Reconfigured metabolism brain network in asymptomatic microtubule-associated protein tau mutation carriers: a

graph theoretical analysis. *Alzheimers Res Ther*. 2022;14(1):52. doi:10.1186/s13195-022-01000-z
27. Chu M, Jiang D, Liu L, et al. Altered anterior insular metabolic connectivity in asymptomatic MAPT P301L carriers. *J Alzheimers Dis*. 2023;93(4):1369-1380. doi:10.3233/JAD-221035
28. Zhang L, Flagan TM, Häkkinen S, et al. Network connectivity alterations across the mutation clinical spectrum. *Ann Neurol*. 2023;94(4):632-646. doi:10.1002/ana.26738
29. Rohrer JD, Nicholas JM, Cash DM, et al. Presymptomatic cognitive and neuroanatomical changes in genetic frontotemporal dementia in the Genetic Frontotemporal dementia Initiative (GENFI) study: a cross-sectional analysis. *Lancet Neurol*. 2015;14(3):253-262. doi:10.1016/S1474-4422(14)70324-2
30. Miyagawa T, Brushaber D, Syrjanen J, et al. Utility of the global CDR® plus NACC FTLD rating and development of scoring rules: data from the ARTFL/LEFFTDS Consortium. *Alzheimers Dement J Alzheimers Assoc*. 2020;16(1):106-117. doi:10.1002/alz.12033
31. Fischl B. FreeSurfer. *NeuroImage*. 2012;62(2):774-781. doi:10.1016/j.neuroimage.2012.01.021
32. Routier A, Burgos N, Díaz M, et al. Clinica: an open-source software platform for reproducible clinical neuroscience studies. *Front Neuroinformatics*. 2021;15:689675. doi:10.3389/fninf.2021.689675
33. Fischl B, Dale AM. Measuring the thickness of the human cerebral cortex from magnetic resonance images. *Proc Natl Acad Sci*. 2000;97(20):11050-11055. doi:10.1073/pnas.200033797
34. Le Du V, DWEZ [Computer software]. https://github.com/Vince-LD/DWEZ Published online 2023.
35. Wasserthal J, Neher P, Maier-Hein KH. TractSeg—Fast and accurate white matter tract segmentation. *NeuroImage*. 2018;183:239-253. doi:10.1016/j.neuroimage.2018.07.070
36. Esteban O, Markiewicz CJ, Blair RW, et al. fMRIPrep: a robust preprocessing pipeline for functional MRI. *Nat Methods*. 2019;16(1):111-116. doi:10.1038/s41592-018-0235-4
37. Schaefer A, Kong R, Gordon EM, et al. Local-global parcellation of the human cerebral cortex from intrinsic functional connectivity MRI. *Cereb Cortex*. 2018;28(9):3095-3114. doi:10.1093/cercor/bhx179
38. Hong SJ, Xu T, Nikolaidis A, et al. Toward a connectivity gradient-based framework for reproducible biomarker discovery. *NeuroImage*. 2020;223:117322. doi:10.1016/j.neuroimage.2020.117322
39. Dopper EGP, Rombouts SARB, Jiskoot LC, et al. Structural and functional brain connectivity in presymptomatic familial frontotemporal dementia. *Neurology*. 2014;83(2):e19-e26. doi:10.1212/WNL.0000000000000583
40. Cash DM, Bocchetta M, Thomas DL, et al. Patterns of gray matter atrophy in genetic frontotemporal dementia: results from the GENFI study. *Neurobiol Aging*. 2018;62:191-196. doi:10.1016/j.neurobiolaging.2017.10.008
41. Chu SA, Flagan TM, Staffaroni AM, et al. Brain volumetric deficits in MAPT mutation carriers: a multisite study. *Ann Clin Transl Neurol*. 2021;8(1):95-110. doi:10.1002/acn3.51249
42. Domínguez-Vivero C, Wu L, Lee S, et al. Structural brain changes in preclinical FTD MAPT mutation carriers. *J Alzheimers Dis*. 2020;75(2):595-606. doi:10.3233/JAD-190820
43. Bocchetta M, Todd EG, Bouzigues A, et al. Structural MRI predicts clinical progression in presymptomatic genetic frontotemporal dementia: findings from the GENetic Frontotemporal dementia Initiative cohort. *Brain Commun*. 2023;5(2):fcad061. doi:10.1093/braincomms/fcad061
44. Jiskoot LC, Bocchetta M, Nicholas JM, et al. Presymptomatic white matter integrity loss in familial frontotemporal dementia in the GENFI cohort: a cross-sectional diffusion tensor imaging study. *Ann Clin Transl Neurol*. 2018;5(9):1025-1036. doi:10.1002/acn3.601
45. Panman JL, Jiskoot LC, Bouts MJRJ, et al. Gray and white matter changes in presymptomatic genetic frontotemporal dementia: a longitudinal MRI study. *Neurobiol Aging*. 2019;76:115-124. doi:10.1016/j.neurobiolaging.2018.12.017
46. Moore K, Convery R, Bocchetta M, et al. A modified Camel and Cactus Test detects presymptomatic semantic impairment in genetic frontotemporal dementia within the GENFI cohort. *Appl Neuropsychol Adult*. 2020;0(0):1-8. doi:10.1080/23279095.2020.1716357
47. Bouzigues A, Russell LL, Peakman G, et al. Anomia is present presymptomatically in frontotemporal dementia due to MAPT mutations. *J Neurol*. 2022;269(8):4322-4332. doi:10.1007/s00415-022-11068-0
48. Poos JM, Russell LL, Peakman G, et al. Impairment of episodic memory in genetic frontotemporal dementia: a GENFI study. *Alzheimers Dement Diagn Assess Dis Monit*. 2021;13(1):e12185. doi:10.1002/dad2.12185
49. Poos JM, Moore KM, Nicholas J, et al. Cognitive composites for genetic frontotemporal dementia: gENFI-Cog. *Alzheimers Res Ther*. 2022;14(1):10. doi:10.1186/s13195-022-00958-0
50. Feis RA, Bouts MJRJ, Dopper EGP, et al. Multimodal MRI of grey matter, white matter, and functional connectivity in cognitively healthy mutation carriers at risk for frontotemporal dementia and Alzheimer's disease. *BMC Neurol*. 2019;19(1):343. doi:10.1186/s12883-019-1567-0
51. Chen Q, Boeve BF, Schwarz CG, et al. Tracking white matter degeneration in asymptomatic and symptomatic *MAPT* mutation carriers. *Neurobiol Aging*. 2019;83:54-62. doi:10.1016/j.neurobiolaging.2019.08.011
52. Corriveau-Lecavalier N, Tosakulwong N, Lesnick TG, et al. Neurite-based white matter alterations in MAPT mutation carriers: a multi-shell diffusion MRI study in the ALLFTD consortium. *Neurobiol Aging*. 2024;134:135-145. doi:10.1016/j.neurobiolaging.2023.12.001
53. Agosta F, Basaia S, Spinelli EG, et al. Modelling pathological spread through the structural connectome in the frontotemporal dementia clinical spectrum. *Brain*. 2025;148(6):1994-2007. doi:10.1093/brain/awae391
54. Frost B, Ollesch J, Wille H, Diamond MI. Conformational diversity of wild-type Tau fibrils specified by templated conformation change. *J Biol Chem*. 2009;284(6):3546-3551. doi:10.1074/jbc.M805627200
55. Sima AAF, Defendini R, Keohane C, et al. The neuropathology of chromosome 17-linked dementia. *Ann Neurol*. 1996;39(6):734-743. doi:10.1002/ana.410390609
56. Ling H, Kovacs GG, Vonsattel JPG, et al. Astrogliopathy predominates the earliest stage of corticobasal degeneration pathology. *Brain*. 2016;139(12):3237-3252. doi:10.1093/brain/aww256
57. Jackson J, Bianco G, Rosa AO, et al. White matter tauopathy: transient functional loss and novel myelin remodeling. *Glia*. 2018;66(4):813-827. doi:10.1002/glia.23286
58. Sahara N, Perez PD, Lin WL, et al. Age-related decline in white matter integrity in a mouse model of tauopathy: an in vivo diffusion tensor magnetic resonance imaging study. *Neurobiol Aging*. 2014;35(6):1364-1374. doi:10.1016/j.neurobiolaging.2013.12.009
59. Whitwell JL, Josephs KA, Avula R, et al. Altered functional connectivity in asymptomatic MAPT subjects. *Neurology*. 2011;77(9):866-874. doi:10.1212/WNL.0b013e31822c61f2
60. Lin LC, Nana AL, Hepker M, et al. Preferential tau aggregation in von Economo neurons and fork cells in frontotemporal lobar degeneration with specific MAPT variants. *Acta Neuropathol Commun*. 2019;7(1):159. doi:10.1186/s40478-019-0809-0
61. Whiteside DJ, Holland N, Tsvetanov KA, et al. Synaptic density affects clinical severity via network dysfunction in syndromes associated with frontotemporal lobar degeneration. *Nat Commun*. 2023;14(1):8458. doi:10.1038/s41467-023-44307-7
62. Carrera E, Tononi G. Diaschisis: past, present, future. *Brain*. 2014;137(9):2408-2422. doi:10.1093/brain/awu101
63. Rytty R, Nikkinen J, Paavola L, et al. GroupICA dual regression analysis of resting state networks in a behavioral variant of frontotemporal dementia. *Front Hum Neurosci*. 2013;7:461. doi:10.3389/fnhum.2013.00461

64. Chiong W, Wilson SM, D'Esposito M, et al. The salience network causally influences default mode network activity during moral reasoning. *Brain*. 2013;136(6):1929-1941. doi:10.1093/brain/awt066
65. Caminiti SP, Canessa N, Cerami C, et al. Affective mentalizing and brain activity at rest in the behavioral variant of frontotemporal dementia. *NeuroImage Clin*. 2015;9:484-497. doi:10.1016/j.nicl.2015.08.012
66. Finger E, Malik R, Bocchetta M, et al. Neurodevelopmental effects of genetic frontotemporal dementia in young adult mutation carriers. *Brain*. 2023;146(5):2120-2131. doi:10.1093/brain/awac446
67. Hefti MM, Farrell K, Kim S, et al. High-resolution temporal and regional mapping of MAPT expression and splicing in human brain development. *PLoS One*. 2018;13(4):e0195771. doi:10.1371/journal.pone.0195771
68. Brion JP, Smith C, Couck AM, Gallo JM, Anderton BH. Developmental changes in τ phosphorylation: fetal τ is transiently phosphorylated in a manner similar to paired helical filament-τ characteristic of Alzheimer's disease. *J Neurochem*. 1993;61(6):2071-2080. doi:10.1111/j.1471-4159.1993.tb07444.x
69. Tsvetanov KA, Gazzina S, Jones PS, et al. Brain functional network integrity sustains cognitive function despite atrophy in presymptomatic genetic frontotemporal dementia. *Alzheimers Dement*. 2021;17(3):500-514. doi:10.1002/alz.12209
70. Rittman T, Borchert R, Jones S, et al. Functional network resilience to pathology in presymptomatic genetic frontotemporal dementia. *Neurobiol Aging*. 2019;77:169-177. doi:10.1016/j.neurobiolaging.2018.12.009
71. Kim EJ, Hwang JHL, Gaus SE, et al. Evidence of corticofugal tau spreading in patients with frontotemporal dementia. *Acta Neuropathol (Berl)*. 2020;139(1):27-43. doi:10.1007/s00401-019-02075-z
72. Roemer-Cassiano SN, Wagner F, Evangelista L, et al. Amyloid-associated hyperconnectivity drives tau spread across connected brain regions in Alzheimer's disease. *Sci Transl Med*. 2025;17(782):eadp2564. doi:10.1126/scitranslmed.adp2564
73. Gordon E, Rohrer JD, Fox NC. Advances in neuroimaging in frontotemporal dementia. *J Neurochem*. 2016;138(S1):193-210. doi:10.1111/jnc.13656
74. Schaffler-Schaden D, Krutter S, Seymer A, Eßl-Maurer R, Flamm M, Osterbrink J. Caring for a relative with dementia: determinants and gender differences of caregiver burden in the rural setting. *Brain Sci*. 2021;11(11):1511. doi:10.3390/brainsci11111511
75. Young AL, Bocchetta M, Russell LL, et al. Characterizing the clinical features and atrophy patterns of MAPT-Related frontotemporal dementia with disease progression modeling. *Neurology*. 2021;97(9):e941-e952. doi:10.1212/WNL.0000000000012410

SUPPORTING INFORMATION

Additional supporting information can be found online in the Supporting Information section at the end of this article.

How to cite this article: Bouzigues A, Du VL, Joulot M, et al. Structural and functional connectivity in tau mutation carriers: from presymptomatic to symptomatic frontotemporal dementia. *Alzheimer's Dement*. 2025;21:e70367. https://doi.org/10.1002/alz.70367